Journal of Environmental Chemical Engineering 3 (2015) 1555–1561

Contents lists available at ScienceDirect

Journal of Environmental Chemical Engineering

journal homepage: www.elsevier.com/locate/jece

Removal of chromium(VI) using nano-hydrotalcite/SiO_2 composite

Eduardo Pérez[a], Lijalem Ayele[a], Girum Getachew[a], Geolar Fetter[b], Pedro Bosch[a,c], Alvaro Mayoral[d], Isabel Díaz[a,e,*]

[a] Chemistry Department, Addis Ababa University, Addis Ababa, Ethiopia
[b] Facultad de Ciencias Químicas, Benemérita Universidad Autónoma de Puebla, Puebla,Mexico
[c] Instituto de Investigaciones en Materiales, Universidad Nacional Autónoma de México, Mexico
[d] Advanced Microscopy Laboratory (LMA), Nanoscience Institute of Aragon (INA), University of Zaragoza, Mariano Esquillor, Edificio I+D, 50018 Zaragoza, Spain
[e] Instituto de Catálisis y Petroleoquímica, CSIC, c/Marie Curie 2, 28049 Madrid, Spain

ARTICLE INFO

Article history:
Received 31 March 2015
Accepted 12 May 2015
Available online 16 May 2015

Keywords:
Hydrotalcite
Nano-hydrotalcite
Memory effect
Chromium
Anion exchange

ABSTRACT

Nano-hydrotalcite (nano-HT), particles have been supported on silica and tested for chromium(VI) retention through anion exchange mechanism. Ultra high resolution has been achieved in the structural characterization of the nano-hydrotalcite particles allowing identification of the Cr within few layers of the nanoparticles. Compared to a reference hydrotalcite (HT), in which the Cr(VI) retention takes place via memory effect, nano-HT/SiO_2 exhibits better adsorption capacity, for 4 mg/L Cr(VI) solutions, even when the adsorption mechanism of the later is anion exchange. This higher adsorption capacity can be attributed to the considerable smaller size of the crystals, which would favor adsorption kinetics and would minimize possible hindrances between the layers of hydrotalcite. The adsorption behavior of nano-HT/SiO_2 can be described by a Freundlich isotherm suggesting a non-uniform surface, which is consistent to their arrangement in nanocrystallites observed by TEM.

Introduction

Environmentally hazardous wastewaters from tannery industry are among the most polluted either due to chromium as well as to organic residues [1]. Indeed, the most polluting species are the chromates formed with chromium(VI) and chromium(III) cation. Cr(VI) exposure causes marked irritation of the respiratory track and ulceration and perforation of the nasal septum in workers in the chromate producing and using industries and it may induce cancer [2]. The maximum levels permitted in drinking water are 5 mg/L for trivalent and 0.05 mg/L for hexavalent chromium. The tolerance limit for Cr(VI) for discharge into inland surface waters is 0.1 mg/L and in potable water is 0.05 mg/L. Therefore, among heavy metal ions, chromium requires considerable attention.

The cleaning of such sludge has been proposed using membrane filtration [3], chemical agents and precipitation [4], ion exchange resins [5] among many others. However, these techniques are costly, energy-intensive and not efficient for low concentrations. Nowadays, adsorption onto porous solids is receiving increasing attention for Cr(VI) removal because its effectiveness and low-cost. Many adsorbents have been proposed such as inorganic solids, active carbon, biosorbents and lignocellulosic materials among others [6–8]. Furthermore there is a possibility to recover the metal or even the retained chromium to be disposed for some useful application such as catalysis [9,10].

An original and recent approach has been the use of ionic exchangers such as hydrotalcites (HT) [11–15]. Hydrotalcites, also known as layered double hydroxides (LDH), are anionic clays with positively charged octahedral hydroxide layers, which are neutralized by interlayer anions and water molecules, and which are generally formulated as $[M^{2+}_{1-x}M^{3+}_{x}(OH)_2]$ $(A^{m-})_{x/m}\cdot nH_2O$, where M^{2+} and M^{3+} are di- and tri-valent cations, respectively, A^{m-} is an anion whose charge is $m-$. Magnesium–aluminum hydrotalcite with the formula $[Mg_6Al_2(OH)_{16}]^{2+}\cdot CO_3^{2-}\cdot 4H_2O$, and a layered structure is stable up to 400 °C. They are structurally formed by brucite-like ($Mg(OH)_2$) sheets where isomorphous substitution of Mg^{2+} by a trivalent cation like Al^{3+} produces a positive charge in the layer that is compensated by anions, which occupy the interlayer space along with water molecules. Hidrotalcite-like materials with similar properties can be obtained by substituting Mg^{2+} by other divalent cation keeping the same structure. The cation nature, the ratio M^{3+}/M^{2+}, the synthesis method, among others determine the properties of the layered

* Corresponding author at: Instituto de Catálisis y Petroleoquímica, CSIC, c/ Marie Curie 2, 28049 Madrid, Spain. Tel.: +34 915 854785.
E-mail address: idiaz@icp.csic.es (I. Díaz).

http://dx.doi.org/10.1016/j.jece.2015.05.009
2213-3437/

double hydroxides [16,17]. Hydrotalcites, as many clays, may be expanded introducing compounds between the layers [18]. The interlayer spaces in carbonate and nitrate exchanged hydrotalcites are either 2.9 or 4.0 Å, respectively. One of the most exploited properties of hydrotalcites is the so called "memory effect" which consists in the spontaneous structural reconstruction of the original layered structure after being calcined and then put in water or aqueous solutions containing different anions [19–21].

There are generally two mechanisms for adsorption of chromate in HT, the first of them is the already mentioned, memory effect, where the HT is calcined at high temperatures, i.e., 350–800 °C for several hours, resulting in mixed metal oxide which is more precisely a solid solution of the two metal oxides. The layer structure is lost during the calcination. When this material is put in contact to an Cr(VI) aqueous solution, the HT recovers its layered structure and the chromate anions are trapped within the HT layers [11,12]. The second mechanism, anion exchange, does not require calcination and it is simply based on equilibrium between the anions within the HT layers and the bulk solution.

Memory effect mechanism generally is much more efficient than anion exchange, giving adsorption capacities for Cr(VI) ca. 10 times higher than the latter [13]. However, memory effect largely depends on many factors, such as the HT composition and the calcination temperature [14,15]. As an example, when calcination temperature is as low as 350 °C, the adsorption of Cr (VI) in HT-like compounds by memory effect is comparable to that by anion exchange [14]. It is obvious that, from the point of view of simplicity and energy-efficiency, it would be desirable to find an alternative to the calcination step for example, by increasing the adsorption capacity by anion exchange of the materials. One possible approach could be by reducing the size of HT particles to nanometric dimensions (nano-HT). Nanostructured HT materials are receiving growing interest to enhance the properties of bulk HT for its applications in photocatalysis, heterogeneous catalysis and adsorption [22]. However, the active sites in these new materials are required to possess enough stability to assure long-term use and recyclability [23]. One well-known approach is to disperse nanoparticles onto different support materials to avoid aggregation. In the case of adsorption, nanostructured HT supported on different substrates have shown enhanced adsorption capacities for dyes [24] and Cr(VI) [25].

Silica (SiO_2) is often utilized as catalyst support. Indeed, it is inactive and it presents a very high specific surface area and tunable porosity. Furthermore, it is thermally stable. The purpose of this work is then to prepare nano-hydrotalcite particles supported on silica and to test them in Cr(VI) retention through anion exchange mechanism. The reference HT sample will be presented in order to compare with memory effect mechanism. Furthermore, atomic level has been achieved in the structural characterization of the nano-hydrotalcite particles allowing identification of the Cr within few layers of the particles. An adsorption study is presented using the nano-hydrotalcite/SiO_2 composite.

Materials and methods

HT and HT/SiO_2 preparation

SBA-15 was used as SiO_2 support in the synthesis of nano-hydrotalcite (nano-HT) [26], 10.5 g of calcined SBA-15 [27] were dispersed in NaOH (2 M) and aluminum and magnesium nitrates solutions (2.5 M) in 50 mL of distilled water. The reactive amounts were calculated for a molar ratio Mg/Al = 3 and SiO_2/HT = 7/3 (w/w). The mixture was treated in a microwave autoclave at 80 °C and 200 W for 10 min (MIC-I Sistemas y Equipos de Vidrio S.A. de C.V.). This procedure of crystallization, i.e., in a closed reactor and in a very short time (10 min), guarantees that no contamination with inter-layered carbonate occurs. In this way, nitrates and hydroxyls, from the reagents, may be expected as compensating anions between the layers. A stirring mechanism is adapted to the reactor to maintain constant temperature [28]. The solids were recovered by decantation and washed several times with distilled water and dried in an oven at 70 °C overnight. For comparison purposes, a conventional HT was prepared with Mg:Al 3:1 following the procedure described by Tichit et al. [29]. In this work, the HT sample was calcined at 500 °C for 8 h in order to destroy the layered structure prior to the adsorption of Cr(VI) via memory effect.

Characterization

Powder X-ray diffraction (XRD) patterns were collected with a Philips X'PERT diffractometer equipped with an X'Celerator detector and using Cu Kα radiation. Scanning transmission electron microscopy (STEM) was performed in a spherical aberration corrected FEI Titan XFEG which was operated at 300 kV equipped with a corrector for the electron probe allowing a maximum resolution of 0.8 Å, the microscope was also equipped with an EDS detector (EDAX) and a Gatan Tridiem energy filter. Prior observations the samples were crushed, dispersed and placed onto a holey carbon copper microgrid. Inductively coupled plasma optical emission spectrometry, (ICP-OES) (Optima 3300 DV model) was used to determine chemical weight percent composition of the samples. Total Chromium for the control experiment was determined by an Analitik Jena ZEEnit 700 P Atomic Absorption Spectrometer.

Chromium adsorption experiments

Chromate starting solutions were prepared by dilution of the corresponding amount of $K_2Cr_2O_7$ salt in distilled water. For the comparative studies of HT and nano-HT/SiO_2, 2.5 mL of 4 mg/L Cr (VI) solution and the corresponding amount of adsorbent were placed in a vial. All the dosage rates were based on weight of adsorbent, i.e. including the SiO_2 support in the composite. For the adsorption isotherm experiments 20 mg of nano-HT/SiO_2 and 20 mL of Cr(VI) solution (adsorbent dose 1 g/L) at different concentrations were placed in a beaker. All the mixtures were stirred using a magnetic stirrer for a contact time of 24 h. After adsorption, the mixture was centrifuged and the supernatant is analyzed for Cr(VI) concentration. The starting solutions were also analyzed in each case. Adsorption removal (%rem) was calculated using the following expression:

$$\%\text{rem} = \frac{c_{eq}}{c_0} \times 100 \quad (1)$$

where c_{eq} is the concentration of Cr(VI) after equilibrium is reached and c_0 is the starting concentration. In order to be sure that all the Cr(VI) has been removed from the solution by adsorption instead of other parallel mechanisms (such as Cr(VI) degradation), the remaining solution of an adsorption experiment (c_0 = 30 mg/L, adsorbent dose = 1 g/L) was analyzed for total chromium by atomic absorption spectrometry. This control experiment revealed that the concentration of total chromium matched to concentration of Cr(VI) by UV–vis spectrophotometry within experimental error, indicating that no degradation occurred.

Cr(VI) UV–vis spectrophotometry analysis

Chromium(VI) concentration was measured using a UV–vis spectrometer (PerkinElmer UV WinLab 6.0.3.0730/1.61.00 Lambda 900) using the EPA method 7196A [30]. In order to improve sensitivity, the sample is treated with the complexation agent, 1, 5-

diphenyl carbazide (DPC) in acidic medium. 2.5 mL of DPC solution (0.25 g/L) and 0.5 mL of H_2SO_4 0.1 mol/L were added to 10 mL of Cr (VI) sample. At least 30 min is needed until all the violet complex Cr (VI)-DPC was formed. Dilution was accurately taken into account by weighing the amounts of each component with a precision of four decimal figures. The UV–vis spectra of the mixtures were then measured in a 1 cm quartz cell and maximum absorbance (540–542 nm) was recorded. For the calibration, a 100 mg/L stock solution was initially prepared by diluting 0.283 g of $K_2Cr_2O_7$ in 1 L distilled water. Calibrant solutions were prepared by dilution of the latter. A calibration line was built (7 points, up to 2 mg/L Cr(VI)) yielding a slope with an uncertainty better than 1%. Cr(VI) concentrations for all the solutions were analyzed following the method above. Whenever necessary they were diluted to a concentration lying within the calibration range. If the amount of sample is less than 10 mL, amount of DPC and H_2SO_4 added are reduced proportionally. Calibration slope and dilution factors were used to convert absorbance into Cr(VI) concentration.

Results and discussion

Structural study of HT and nano-HT/SiO_2

The nature of the adsorption mechanism could be initially characterized by X-ray diffraction of the solids before and after exposing them to the CrO_4^{2-} solution (Fig. 1). The memory effect when using HT vs. the anion exchange route followed by nano-HT/SiO_2 could be explained following the structure of the layers in both cases. Fig. 1a collects the XRD patterns of conventional HT after calcination, and upon CrO_4^{2-} removal. The profile of HT calcined at 500 °C shows the loss of the layered structure, showing intensities due to the crystalline mixed oxide formed upon the collapse of the layers. When the HT calcined is exposed to a water solution of Cr(VI) the spontaneous structural reconstruction of the original layered structure takes place due to the adsorption of the CrO_4^{2-} anions that become the scaffold for the cationic layers. The XRD profile of HT exposed to 4 mg/L of Cr(VI) solution at 1 g/L of adsorbent dose can be indexed to the typical layered structure of hydrotalcite. The presence of Cr in this solid could be corroborated by ICP giving 0.24 wt% Cr.

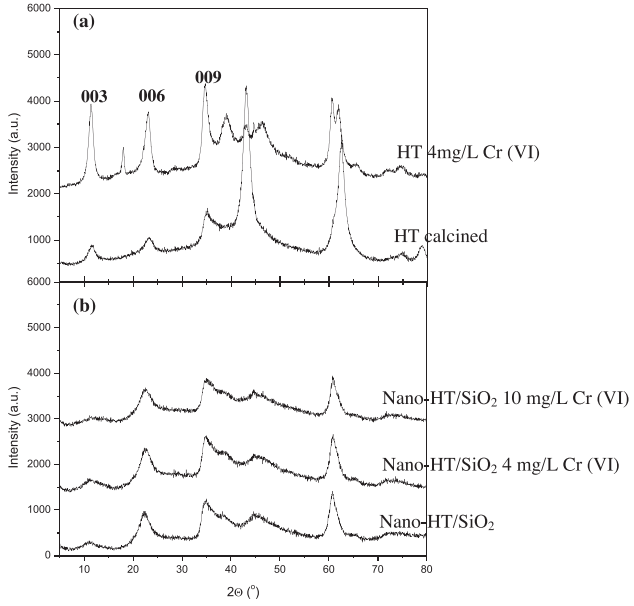

Fig. 1. X-ray diffraction patterns of HT (a) and nano-HT/SiO_2 (b) before and after chromium removal.

In the case of the composite the nanometric nature of the HT is envisaged by the presence of broad diffraction peaks with very low intensity (Fig. 1b). The high background is also indicative of the amorphous nature of the SiO_2 support with no diffraction observed at low angle, which corroborates that the initial SBA-15 structure is no longer hexagonal after the synthesis of the nano-HT. Nevertheless, since this material is not calcined prior de adsorption experiment, there is no change in the overall profile. On the contrary, the XRD profile is identical after adsorption of 4 or 10 mg/L of chromate anions at 1 g/L adsorbent dose. The profiles could be indexed again as the layered structure of HT, and the presence of identical structure before and after adsorption experiment corroborates that in this case, the mechanism is by anion exchange with no change in the d-spacing between the layers. Once again, the presence of Cr in these solids could be corroborated by elemental analyses (ICP), obtaining 0.38 wt% in the 4 mg/L experiment and 1.29 wt% Cr in nano-HT/$SiO_2$10 mg/L.

Further electron microscopy studies were carried out in order to understand the nature of the composite. Spherical aberration (C_s) corrected Scanning Transmission Electron Microscopy coupled with High Angular Annular Dark Field detector (C_s-corrected STEM-HAADF) instead of conventional TEM was chosen due to the high analytical power of this mode, while maintaining atomic resolution thanks to the C_s corrector in the condenser system. Besides, it has to be mentioned that HT are extremely unstable under the electron beam due to the large amount of water contained in the layered structure, thus, a precise control on the exposure to the electron beam has to be taken into account [31–33].

This mode yields to images with dark background, while the solid shows light contrast, and thus the brighter areas are commonly directly related to the higher atomic number of the elements. Low magnification STEM-HAADF images already allow observing different morphology of the particles forming the adsorbent. In the case of conventional HT (Fig. 2a), the particles are uniform and rather large, although in the composite sample (Fig. 2b), within the same range of magnification, it is possible to observe the agglomerated nature of the particles, showing an uneven surface and morphology. A closer look to conventional HT reveals uniform crystals (Fig. 3a) with layered structure with d-spacings of 0.64 nm (Fig. 3b). The microscopy study was carried out after Cr(VI) removal in 4 mg/L solution, thus small amount of Cr could be detected by EDS, although the layered structure analyzed seems to be perfectly recovered after calcination, proving the memory effect mechanism. Fig. 4a and b show the high magnification images of nano-HT/SiO_2 in which due to the high-resolution achieved three layers with d-spacing of 0.62 nm (Fig. 4a) can be observed. Given the lack of stability of these materials, this result implies an unprecedented high resolution imaging of hydrotalcites most probably due to the strength provided by the SiO_2 support. EDS analyses was conducted in the area imaged as Fig. 4b, yielding the Mg, Al in the ratio expected by the HT structure, and Si coming from the support, as well as Cr in a higher amount than before since this sample was observed after 10 mg/L adsorption experiment.

Chromium adsorption studies of HT and nano-HT/SiO_2

Table 1 shows the adsorption removal (%rem) of HT and nano-HT/SiO_2 for a 4 mg/L solution of Cr(VI) at different dosage rates. The Cr(VI) removal is significantly high for both adsorbents even at low dosage rates. For 10 g/L the adsorption removal is 100% in both cases but upon decreasing the dosage rate to 1 g/L the adsorption removal is only decreased down to 85.4% for HT and 94.6% for nano-HT/SiO_2. Similar results are obtained by Lazaridis and Asouhidou [34] for dosage rates ranging from 0.2 to 0.5 mg/L.

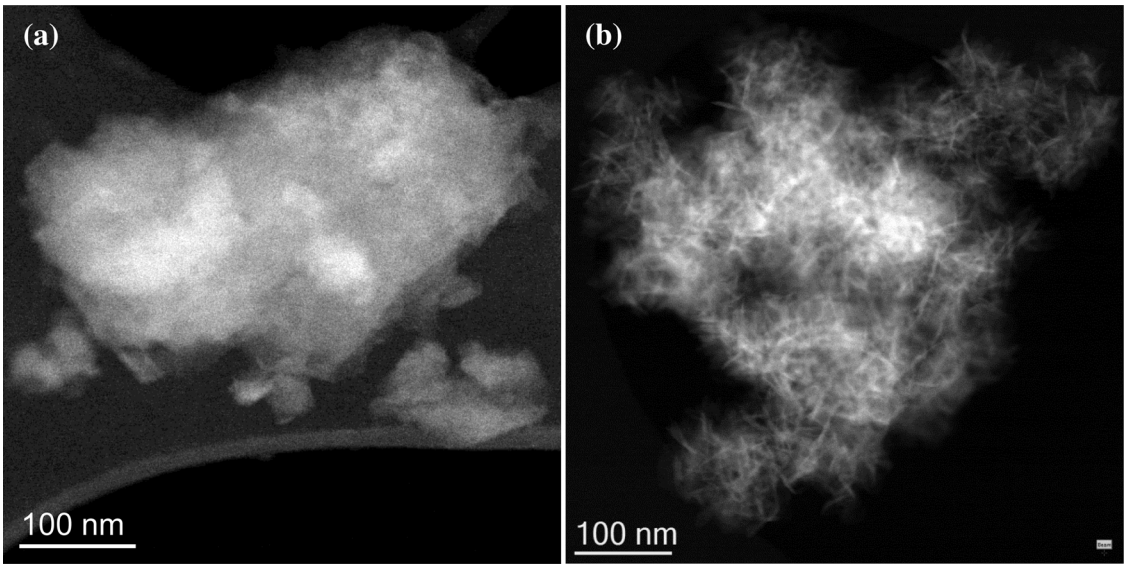

Fig. 2. C_s-corrected STEM-HAADF low magnification images of HT (a) and nano-HT/SiO_2 (b).

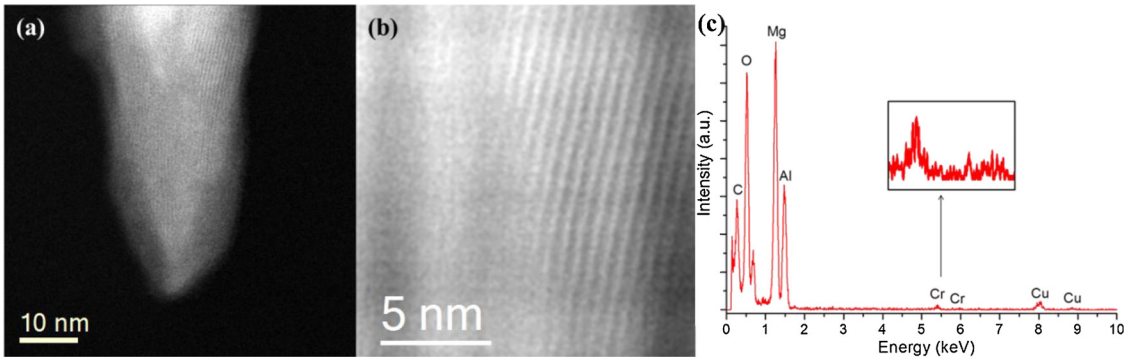

Fig. 3. (a) C_s-corrected STEM-HAADF image of the HT particle where the chemical analysis was performed. (b) A closer look into the HT showing the layers that form the structure with interlayer d-spacing of 0.64 nm. (c) EDS spectrum which displays the HT composition, Al, Mg and O, and corroborates the absorption of Cr.

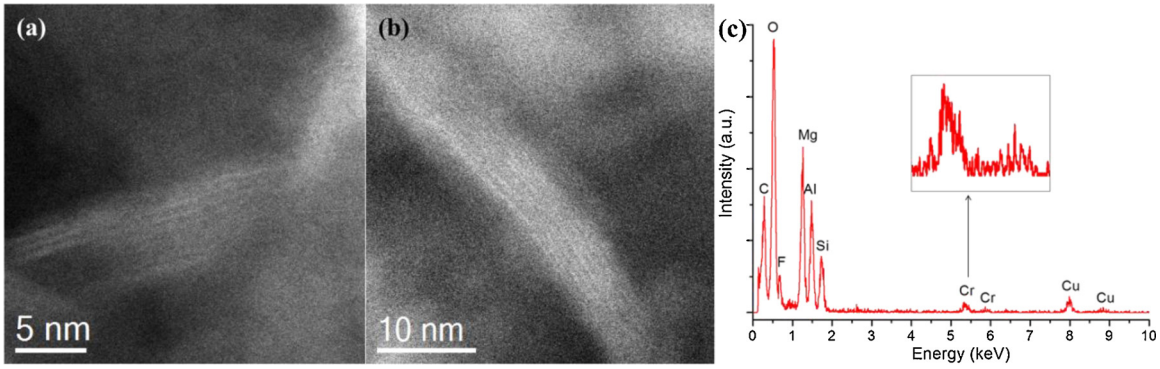

Fig. 4. (a) and (b) High-resolution images of 50 nm nano-HT/SiO_2 crystals revealing the interlayer d-spacing of 0.62 nm. (c) EDS spectrum which displays the composition of the composite: Si, Al, Mg and O, and corroborates the absorption of Cr.

Table 1
Adsorption removal (%) of HT and nano-HT/SiO_2 for a 4 mg/L solution of Cr(VI) at different dosage rates.

Dosage rate	Adsorption removal (%)			
	10 (g/L)	5 (g/L)	2 (g/L)	1 (g/L)
HT	100	88.7	87.8	85.4
nano-HT/SiO_2	100	98.6	96.3	94.6

Initial Cr(VI) concentration of 10 mg/L and a similar adsorbent composition and calcination temperature. However, it is possible to observe that nano-HT/SiO_2 exhibits better adsorption capacity than HT, for the conditions evaluated, even when the adsorption mechanism of the former is anion exchange. The higher adsorption capacity of the latter can be then attributed to the considerable smaller size of the crystals, which would favor adsorption kinetics and would minimize possible hindrances between the layers of HT. These results are also in agreement with the structural

observations described earlier, and with the amount of Cr detected by ICP in the HT and nano-HT/SiO_2 samples at 1 g/L.

The behavior of the equilibrium of adsorption between adsorbates and adsorbents is usually rationalized by adsorption isotherms, which establish a relationship more or less empirical between the adsorption capacity of the adsorbent (amount of adsorbate retained per mass of adsorbent, q_{eq}) and the concentration of the bulk solution in equilibrium. q_{eq} can be calculated using the following expression:

$$q_{eq} = \frac{(c_{eq} - c_0)V}{m} \quad (2)$$

where V is the volume of solution treated and m the mass of adsorbent utilized.

Two of the most utilized isotherms are the Langmuir isotherm [35] (Eq. (3)) which considers monolayer coverage and uniform surface of the adsorbent, and the empirical Freundlich isotherm [36] (Eq. (4))

$$q_{eq} = \frac{q_m b c_{eq}}{1 + c_{eq}} \quad (3)$$

$$q_{eq} = k_f c_{eq}^{1/n} \quad (4)$$

q_m (maximum adsorption capacity) and b are fitting constants for the Langmuir equation and k_f and n (sorption intensity) are fitting constants for the Freundlich equation.

Fig. 5a shows the adsorption capacity expressed in percent of Cr (VI) removed vs. the initial concentration for a dosage rate of 1 g/L. As expected, for low initial concentrations, the proportion of chromium removed is high (>80%) and it decreases upon increasing initial concentration. The adsorption isotherm is represented in Fig. 5b that plots the relationship between the equilibrium capacity, q_{eq} of the adsorbent (expressed in mg of Cr (VI) per gram of nano-HT/SiO_2) and the concentration of the solution in equilibrium. Representation of $\ln q_e$ vs. $\ln c_e$ fits to a straight line (Fig. 5c), indicating that the data are described by a Freundlich isotherm. From the slope and zero intercept of the fitting the Freundlich parameters can be obtained: $n = 3.5 \pm 0.3$; $k_f = 3.35 \pm 0.14$. The data do not fit to a Langmuir isotherm.

The report by He et al. [25] compares Cr(VI) adsorption of a supported nano-structured HT to adsorption on the same neat HT powder. They fit adsorption data to Langmuir and Freundlich isotherms obtaining values of R^2 higher for the fitting to the former. However, a closer look to the fittings reveals that only the neat HT fits to the Langmuir isotherm whereas the nanostructured material fits to the Freundlich isotherm. The Freundlich constants obtained ($n = 2.24$; $k_f = 3.73$) are comparable to those in this work. The fact that these nanostructured materials do not fit a Langmuir model, suggests a non-uniform surface, which is consistent to their arrangement in nanocrystallites.

Discussion

High anionic exchange capacity and high temperature resistance are the advantages of hydrotalcites compared to organic anionic exchangers. Our results show that calcined hydrotalcites present a high Cr(VI) exchange capacity as already reported in the literature [14,34,37]. However, the morphology or the particle size of hydrotalcite is not often considered although it should explain the variety and high dispersion of values reported in the literature. Such determinations are crucial as adsorption mechanism is not only the exchange of interlayered anions but also adsorption on the external surface and mouth of the layers. In this work, the retention of small hydrotalcite particles supported on SiO_2 is compared to the performance, through the memory effect of calcined hydrotalcites whose resulting particle size is rather large. In order to try to evaluate the possible contribution of sorption on the SiO_2 support, a control experiment was run on a pure silica SBA-15 in similar conditions, showing no removal at all at 2 and 5 g/L. According to these data, the sorption capacity obtained for the composite nano-HT/SiO_2, with 98.6% removal capacity at 5 g/L, could be only due to the nano-HT, and thus, the only way that the HT can remove efficiently is by ion exchange. In this case, through electron microscopy images it was possible to determine the d-spacing after chromium adsorption (0.64 nm) but in the nano-hydrotalcite supported on SiO_2 it turned out to be 0.62 nm for particles whose size is between 5 and 10 nm. The difference between chromium retention on these two materials has, then, to be attributed to the hydrotalcite particle size. At least, it seems that

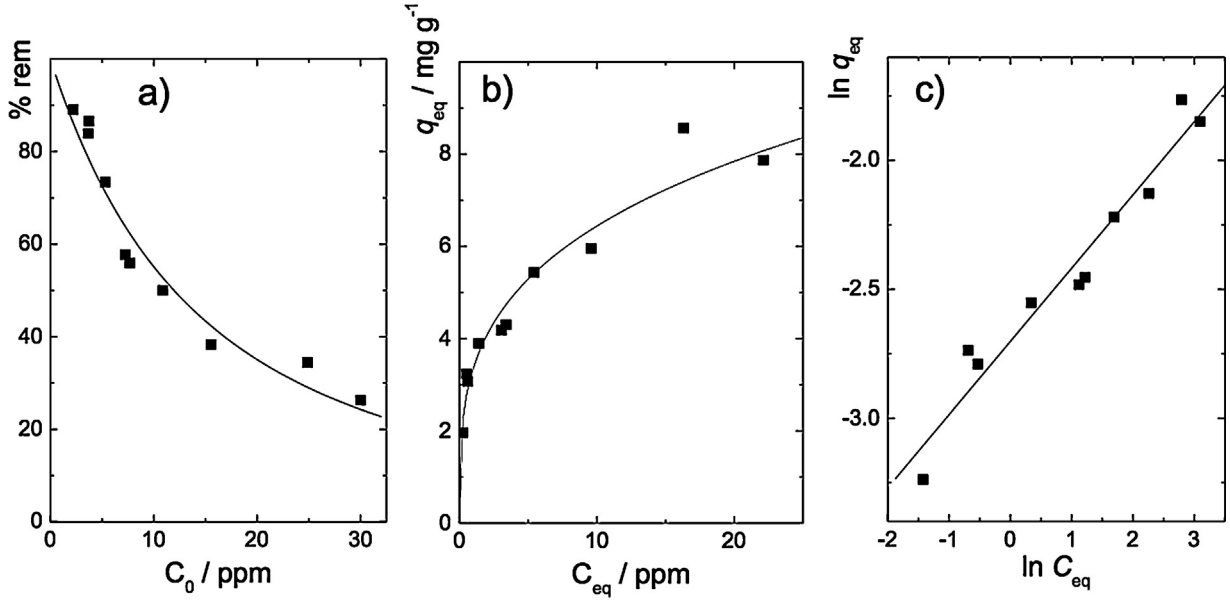

Fig. 5. (a) Cr(VI) % removal from solutions at different concentrations. (b) Adsorption isotherm (q_{eq} vs. equilibrium concentration). (c) Linearized Freundlich adsorption isotherm ($\ln q_e$ vs. $\ln c_{eq}$).

chromium removal may be improved in 10% diminishing particle size with the advantage that no calcination is required. Still, such comparison is reinforced if one takes into account that it corresponds to 1 g of each material but not 1 g of each hydrotalcite; the amount of hydrotalcite present in the nano-HT/SiO_2 should beat most 30%, considering that all hydrotalcite precursors were reacted.

It has to be emphasized that no other report has obtained such high resolution imaging of the corresponding materials. Only in this way it was possible to show the stacking of ca. six layers of hydrotalcite in the 50 nm particles. It seems that due to the presence of SiO_2 during the synthesis, the growth of HT crystals was inhibited or limited, leading to a highly agglomerated composite in which the layers are no larger than six unit cells. Furthermore, the presence of SiO_2 around the HT nanocrystals, although it does not contribute to the retention of chromates, seems to be indirectly favoring the adsorption helping to stabilize the HT nanocrystals.

Conclusions

Mg/Al hydrotalcite structured in crystals of nanometric dimensions supported onto silica (nano-HT/SiO_2) was synthesized and tested for Cr(VI) adsorption from aqueous solutions. The structure and crystal size of the materials has been observed by TEM. Images of hydrotalcite nano-crystals of 5–10 nm and few layers thick have been obtained, which is an unprecedented resolution result. Adsorption of Cr(VI) within the layers of nano-HT has been confirmed by ICP. The nano-HT/SiO_2 adsorbs Cr(VI) by anionic exchange more efficiently than the macroscopic counterpart even though the adsorption mechanism of the latter is by "memory effect". Moreover the inter-layer separation is similar in both cases indicating that the difference between chromium retention on these two materials has to be attributed to the hydrotalcite particle size. A study of adsorption of Cr(VI) onto nano-HT/SiO_2 vs. equilibrium concentration (adsorption isotherm) has been done and the data fit well to the Freundlich isotherm and does not to the Langmuir isotherm, probably due to the non-uniformity of the materials caused by its arrangement in nano-crystals.

Acknowledgements

ID is grateful to CSIC for her research leave at AAU. PB deeply appreciates Universidad Nacional Autónoma de Mexico for supporting him on his sabbatical leave at AAU. The financial support from the Spanish Government MINECO (project MAT2012-31127) and Mexican Government CONACYT is acknowledged. A.M. acknowledges the European Union Seventh Framework Programme under grant agreement 312483—ESTEEM2 (Integrated Infrastructure Initiative—I3).

References

[1] J. Motlagh, J. Eidelson, The Dark Stain on Bangladesh's $1 Billion Leather Export Industry, Bloomberg Businessweek, Global Economics, November 13th, 2014.
[2] B.H. Alexander, H. Checkoway, L. Wechsler, N.J. Heyer, J.M. Muhm, T.P. O'Keeffe, Lung cancer in chromate-exposed aerospace workers, J. Occup. Environ. Med. 38 (12) (1996) 1253–1258, doi:http://dx.doi.org/10.1097/00043764-199612000-00011. 8978517.
[3] A. Aliane, N. Bounatiro, A.T. Cherif, D.E. Akretche, Removal of chromium from aqueous solution by complexation-ultrafiltration using a water-soluble macroligand, Water Res. 35 (9) (2001) 2320–2326, doi:http://dx.doi.org/10.1016/S0043-1354(00)00501-7. 11358314.
[4] M. Gheju, I. Balcu, Removal of chromium from Cr(VI) polluted wastewaters by reduction with scrap iron and subsequent precipitation of resulted cations, J. Hazard. Mater. 196 (2011) 131–138, doi:http://dx.doi.org/10.1016/j.jhazmat.2011.09.002. 21955659.
[5] S. Rengaraj, K.H. Yeon, S.H. Moon, Removal of chromium from water and wastewater by ion exchange resins, J. Hazard. Mater. 87 (1–3) (2001) 273–287, doi:http://dx.doi.org/10.1016/S0304-3894(01)00291-6. 11566415.
[6] B. Saha, C. Orvig, Biosorbents for hexavalent chromium elimination from industrial and municipal effluent, Coord. Chem. Rev. 254 (23–24) (2010) 2959–2972, doi:http://dx.doi.org/10.1016/j.ccr.2010.06.005.
[7] P. Miretzky, A.F. Cirelli, Cr(VI) and Cr(III) removal from aqueous solution by raw and modified lignocellulosic materials: a review, J. Hazard. Mater. 180 (1–3) (2010) 1–19, doi:http://dx.doi.org/10.1016/j.jhazmat.2010.04.060. 20451320.
[8] F. Di Natale, A. Erto, A. Lancia, D. Musmarra, Equilibrium and dynamic study on hexavalent chromium adsorption onto activated carbon, J. Hazard. Mater. 281 (2015) 47–55, doi:http://dx.doi.org/10.1016/j.jhazmat.2014.07.072. 25155159.
[9] S. Kawi, M. Te, MCM-48 supported chromium catalyst for trichloroethylene oxidation, Catal. Today 44 (1–4) (1998) 101–109, doi:http://dx.doi.org/10.1016/S0920-5861(98)00178-3.
[10] H. Yamashita, M. Anpo, Local structures and photocatalytic reactivities of the titanium oxide and chromium oxide species incorporated within micro- and mesoporous zeolite materials: XAFS and photoluminescence studies, Curr. Opin. Solid State Mater. Sci. 7 (6) (2003) 471–481, doi:http://dx.doi.org/10.1016/j.cossms.2004.02.003.
[11] C. Zhao, H.-Y. Zeng, Y.-J. Wang, P.-L. Liu, Y.-Q. Li, Y.-J. Yang, "Memory Effect" Of Mg–Al Hydrotalcites and its Chromium(VI) Adsorption Property, J. Inorg. Mater. 26 (2011) 874–880.
[12] S. Martinez-Gallegos, H. Pfeiffer, E. Lima, M. Espinosa, P. Bosch, S. Bulbulian, Cr (VI) immobilization in mixed (Mg,Al) oxides, Microporous Mesoporous Mater. 94 (1–3) (2006) 234–242, doi:http://dx.doi.org/10.1016/j.micromeso.2006.03.045.
[13] E. Alvarez-Ayuso, H.W. Nugteren, Purification of chromium(VI) finishing wastewaters using calcined and uncalcined Mg–Al–CO_3-hydrotalcite, Water Res. 39 (12) (2005) 2535–2542, doi:http://dx.doi.org/10.1016/j.watres.2005.04.069. 15993462.
[14] E. Ramos-Ramírez, N.L. Ortega, C.A. Soto, M.T. Gutiérrez, Adsorption isotherm studies of chromium(VI) from aqueous solutions using sol–gel hydrotalcite-like compounds, J. Hazard. Mater. 172 (2–3) (2009) 1527–1531, doi:http://dx.doi.org/10.1016/j.jhazmat.2009.08.023. 19744787.
[15] R.L. Goswamee, P. Sengupta, K.G. Bhattacharyya, D.K. Dutta, Adsorption of Cr (VI) in layered double hydroxides, Appl. Clay Sci. 13 (1) (1998) 21–34, doi:http://dx.doi.org/10.1016/S0169-1317(98)00010-6.
[16] F. Cavani, F. Trifirò, A. Vaccari, Hydrotalcite-type anionic clays: preparation, properties and applications, Catal. Today 11 (2) (1991) 173–301, doi:http://dx.doi.org/10.1016/0920-5861(91)80068-K.
[17] V. Rives, Layered Double Hydroxides: Present and Future, Nova Science Publishers, New York, 2001.
[18] G. Fetter, P. Bosch, in: A. Gil, S.A. Korili, R. Trujillano, M.A. Vicente (Eds.), Pillared Clays and Related Catalysts, Springer, New York, 2010, pp. 1–21.
[19] J.C.A.A. Roelofs, A.J. van Dillen, K.P. de Jong, Base-catalyzed condensation of citral and acetone at low temperature using modified hydrotalcite catalysts, Catal. Today 60 (3–4) (2000) 297–303, doi:http://dx.doi.org/10.1016/S0920-5861(00)00346-1.
[20] R.V. Gaines, H.C.W. Skinner, E.E. Ford, B. Mason, A. Rosenzweig, Dana's New Mineralogy, 8th ed., Wiley, New York, 1997.
[21] M.T. Olguín, P. Bosch, D. Acosta, S. Bulbulian, ^{131}I-sorption by thermally treated hydrotalcites, Clays Clay Miner. 46 (5) (1998) 567–573, doi:http://dx.doi.org/10.1346/CCMN.1998.0460510.
[22] S.N. Basahel, S.A. Al-Thabaiti, K. Narasimharao, N.S. Ahmed, M. Mokhtar, Review: nanostructured Mg–Al hydrotalcite as catalyst for fine chemical synthesis, J. Nanosci. Nanotechnol. 14 (2) (2014) 1931–1946. 24749466.
[23] C. Li, M. Wei, D.G. Evans, X. Duan, Layered double hydroxide-based nanomaterials as highly efficient catalysts and adsorbents, Small 10 (22) (2014) 4469–4486, doi:http://dx.doi.org/10.1002/smll.201401464. 25137218.
[24] Y. Zhao, S. He, M. Wei, D.G. Evans, X. Duan, Hierarchical films of layered double hydroxides by using a sol–gel process and their high adaptability in water treatment, Chem. Commun. (Camb.) 46 (17) (2010) 3031–3033, doi:http://dx.doi.org/10.1039/b926906a. 20386858.
[25] S. He, Y. Zhao, M. Wei, D.G. Evans, X. Duan, Fabrication of hierarchical layered double hydroxide framework on aluminum foam as a structured adsorbent for water treatment, Ind. Eng. Chem. Res. 51 (1) (2012) 285–291, doi:http://dx.doi.org/10.1021/ie2015894.
[26] A. Pérez-Verdejo, A. Sampieri, H. Pfeiffer, M. Ruiz-Reyes, J.-D. Santamaría, G. Fetter, Nanoporous composites prepared by a combination of SBA-15 with Mg–Al mixed oxides. Water vapor sorption properties, Beilstein J. Nanotechnol. 5 (2014) 1226–1234, doi:http://dx.doi.org/10.3762/bjnano.5.136. 25161858.
[27] D. Zhao, J. Feng, Q. Huo, N. Melosh, G.H. Fredrickson, B.F. Chmelka, G.D. Stucky, Triblock copolymer syntheses of mesoporous silica with periodic 50 to 300 angstrom pores, Science 279 (5350) (1998) 548–552, doi:http://dx.doi.org/10.1126/science.279.5350.548. 9438845.
[28] J.A. Rivera, G. Fetter, Y. Jiménez, M.M. Xochipa, P. Bosch, Nickel distribution in (Ni,Mg)/Al-layered double hydroxides, Appl. Catal. A 316 (2) (2007) 207–211, doi:http://dx.doi.org/10.1016/j.apcata.2006.09.031.
[29] D. Tichit, A. Rolland, F. Prinetto, G. Fetter, M. de Jesus Martinez-Ortiz, M.A. Valenzuela, P. Bosch, Comparison of the structural and acid–base properties of Ga- and Al-containing layered double hydroxides obtained by microwave irradiation and conventional ageing of the synthesis gels, J. Mater. Chem. 12 (12) (2002) 3832–3838, doi:http://dx.doi.org/10.1039/b203376n.
[30] http://www.epa.gov/osw/hazard/testmethods/sw846/pdfs/7196a.pdf.

[31] I. Diaz, A. Mayoral, TEM studies of zeolites and ordered mesoporous materials, Micron 42 (5) (2011) 512–527, doi:http://dx.doi.org/10.1016/j.micron.2010.12.005. 21227705.
[32] A. Mayoral, J.E. Readman, P.A. Anderson, Aberration-corrected STEM analysis of a cubic Cd array encapsulated in zeolite A, J. Phys. Chem. C 117 (46) (2013) 24485–24489, doi:http://dx.doi.org/10.1021/jp409171q.
[33] A. Mayoral, P.A. Anderson, I. Diaz, Zeolites are no longer a challenge: atomic resolution data by aberration-corrected STEM, Micron 68 (2015) 146–151, doi: http://dx.doi.org/10.1016/j.micron.2014.05.009. 24931385.
[34] N.K. Lazaridis, D.D. Asouhidou, Kinetics of sorptive removal of chromium(VI) from aqueous solutions by calcined Mg–Al–CO_3 hydrotalcite, Water Res. 37 (12) (2003) 2875–2882, doi:http://dx.doi.org/10.1016/S0043-1354(03)00119-2. 12767290.
[35] I. Langmuir, The adsorption of gases on plane surfaces of glass, mica and platinum, J. Am. Chem. Soc. 40 (9) (1918) 1361–1368, doi:http://dx.doi.org/10.1021/ja02242a004.
[36] H. Freundlich, Über die adsorption in losungen, Z. Physiol. Chem. 57 (1906) 387–470.
[37] Y.-B. Zang, W.-G. Hou, W.-X. Wang, Adsorption desorption of chromium VI on Mg–Al hydrotalcite-like compounds, part I. Adsorption, Chin. J. Chem. 65 (2007) 773–778.